

Paper ID: EE23

H6-TYPE IGBT CONFIGURATION FOR SINGLE PHASE GRID CONNECTED TRANSFORMERLESS PHOTOVOLTAIC APPLICATIONS

Ms. Tejal S. Bandgar
M. Tech (Electrical Power System)
Rajarambapu Institute of Technology
Maharashtra, India

Prof. H. T. Jadhav
Professor Electrical Engineering
Rajarambapu Institute of Technology
Maharashtra, India

Abstract—All active switches is presented for a proposed high-efficiency photovoltaic inverter, no isolated, grid connected photovoltaic applications. The proposed H6-type configuration features high efficiency over a wide load range, low ground leakage current, no need for split capacitors, and low-output ac-current distortion. The detailed SPWM scheme, photovoltaic power supply and the power stage of operating principle are described. In this paper not only IGBT, but also MOSFET switch inverter topology explained. The proposed H6 type transformerless inverter topology can be able to reduce strong ground leakage current. The single phase IGBT H6-type transformerless grid connected PV system is simulated using MATLAB/SIMULINK.

Index term— Transformer less inverter; SPWM inverter; Photovoltaic System; Leakage current; Common mode and differential mode characteristics; IGBT Inverter

I. INTRODUCTION

Grid connected transformer less inverter systems are the trend of future PV system because of their more flexibility, easier to installation due to their plug and play nature, and higher system-level energy harnessing capabilities under shaded or PV manufacturing mismatch conditions as compared to the single or multi string inverters[1]–[3]. In the past number of inverter topology has been proposed for the grid connected photovoltaic applications and also the PV ac module applications. In that number of power stages, use of transformers, location of power decoupling capacitors, number of power stages has been proposed for that kind of PV ac module application [4][10]. However this solutions suffer from following drawbacks: 1) limited output range PV panel available in the markets[6]-[7]; 2) limited life of the electrolytic capacitors for the power decoupling [4]-[5]; 3) strong ground leakage current flow due to unipolar pulse width modulation (PWM) scheme used for the grid connected transformerless PV system[8]; 4) high frequency bidirectional converter and low system efficiency[9]-[11]; and 5) increase the complicity and cost of the circuit [12]-[13].

Galvanic isolation for PV application is not required by code a two-stage ac module combining a nonisolated high step-up converter and a high-efficiency inverter with H6-type configuration in an ac module, shown in Fig. 1, can be

used to solve the aforementioned issues. This two-stage system configuration can significantly reduce the power-decoupling capacitance by locating the capacitor in the dc link [2]. And the first stage also can be designed to meet the requirement of the wide input voltage range for the available panels in the market. Reference [14] reported a dc–dc converter with a single active switch combining boost, fly back, and charge-pump circuits to simultaneously achieve wide input range, high-voltage gain, high efficiency, and low cost with the 20–70 V input, 180–200 V output, and 97.4% peak efficiency as the first part of PV integrated ac module. This paper, however, will concentrate on the second power stage—the inverter circuit to obtain high efficiency of the MOSFET dc–ac circuit and to avoid the high ground leakage current issue.

The simplest inverter using hybrid MOSFETs and insulated gate bipolar transistors (IGBTs) with unipolar PWM to achieve high efficiency. The high-side IGBTs serve as line frequency polarity selection switches and low-side MOSFET operate in high frequency sinusoidal PWM (SPWM) to control the output voltage or current. The high efficiency of the hybrid four-switch inverter can be achieved over wide load range because the MOSFETs can avoid the fixed voltage-drop losses and significantly reduce the turn-off losses without tail current as compared to the case with IGBTs. However, the hybrid four-switch inverter with unipolar PWM is not suitable for no isolated ac-module application because the high ground Leakage current is generated through the parasitic capacitance of the PV panel due to the high-frequency voltage swing at the PV terminals. The severe ground leakage current result in the problems, which include lower efficiency, output current distortion, electromagnetic interference (EMI) and safety issue [15][16].

In the given table 1, the leakage current value and the disconnection time in seconds is shows as per the VDE 0126 1-1 standard [17]. This paper is presented as follows: Photovoltaic module with their equations 2. Existing MOSFET H6 type topology 3. Common and differential mode characteristics of the existing topology 3. Ground leakage current detailed 4. Proposed IGBT H6 type topology and 5. Unipolar and bipolar SPWM with CM and DM characteristics.

Paper ID: EE23

TABLE I
LEAKAGE CURRENT RMS AND CORRESPONDING
DISCONNECTION TIMES (DIN VDE 0126-1-1)

Leakage current RMS value	Disconnection Time (s)
30	0.3
60	0.15
150	0.04

II. SYSTEM ANALYSIS

Photovoltaic model is presented using the output and input equations of general mathematical mode. In this current source is in the parallel with diode and the resistor and series with another resistor [3]. The equivalent circuit of the photovoltaic (PV) cell is depicted in the following figure 2.

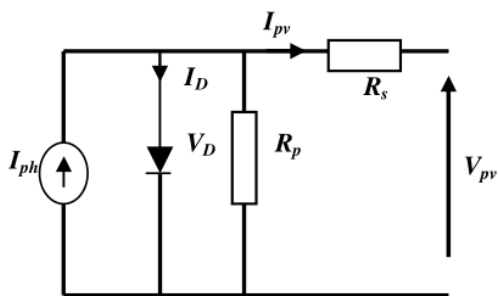


Fig. 1 Equivalent PV cell model

This model is describing the basic equations and C-I characteristics of the photovoltaic cell module are shown in the fig 3

$$0 = I_{ph} - I_D - I_{pv} - \frac{V_{pv} + I_{pv}}{R_p} \quad (1)$$

$$I_D = I_0 (e^{V_D/V_T} - 1) \quad (2)$$

Where:

$$V_D = V_{pv} + I_{pv} \cdot R_s \quad (3)$$

$$V_T = \frac{n \cdot K \cdot T}{q} \quad (4)$$

And :

I_{PV} : The cell current (A)

I_{ph} : The light generated current(A)

I_D : The Shockley diode equation (A).

I_0 : The diode saturation current (A).

R_s : The cell series resistance (Ohms).

R_p : The cell shunt resistance (Ohms).

V_D : The diode voltage (V).

V_T : The temperature voltage (V).

V_{PV} : The cell voltage (V).

n : Dimensionless junction material factor
 K : The Boltzmann constant $1.38 \cdot 10^{-23}$ J/K
 T : The temperature measured by Celsius
 q : The electron charge $1.602 \cdot 10^{-19}$ C

Simplified mathematical model given by Shaowu Li in [3], but the illuminates the second parts “ ΔI ”:

$$I_{pv} = I_{sc} \left[1 - c_1 \left(e^{\frac{V_{pv} - \Delta V}{c_2 \cdot V_{oc}}} - 1 \right) \right] + \Delta I \quad (5)$$

Where:

$$c_1 = \left(1 - \frac{I_m}{I_{sc}} \right) e^{\frac{-V_m}{c_2 \cdot V_{oc}}} \quad (6)$$

$$c_2 = \left(\frac{V_m}{V_{oc}} - 1 \right) / \ln \left(1 - \frac{I_m}{I_{sc}} \right) \quad (7)$$

$$\Delta I = I_{ph} - I_{sc} \quad (8)$$

$$I_{ph} = \frac{E}{E_n} [I_{sc} + K_I \cdot \Delta T] \quad (9)$$

$$\Delta V = R_s \cdot \Delta I - K_V \cdot \Delta T \quad (10)$$

Figure shows the matlab simulink mathematical model of photovoltaic cell model. This is the 400 V photovoltaic matlab model.

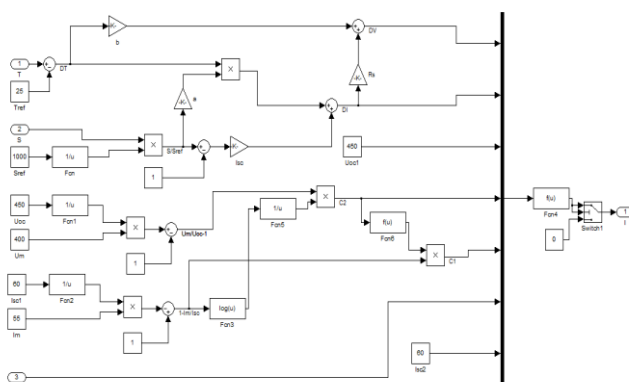


Fig. 2 Matlab model of PV system

Existing MOSFET topology is as shown in the fig. in this system photovoltaic system is connected to the H6 type MOSFET inverter topology. After that the MOSFET inverter is connected to the grid using the filter. Operation of this topology is detailed in the Fig 4. And the modes of operation are detailed in the fig. 5.

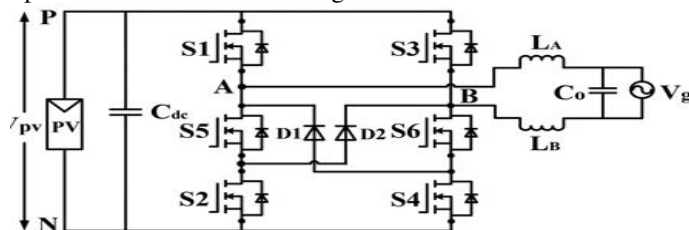


Fig. 3 MOSTET H6 type transformer less topology.

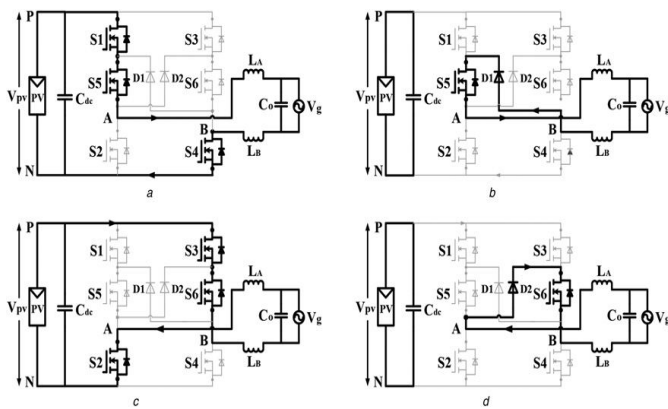


Fig.4 Operation of MOSFET H6 type topology

- A-Active
- B-Freewheeling mode in the positive half-cycle of grid current
- c- Active
- D-Freewheeling mode in the negative half-cycle of grid current

III. PROPOSED INVERTER TOPOLOGY

Proposed topology with H6 type inverter configuration, which consist of six IGBTs (S1 S6), two freewheeling diode (D1 and D2), and filer (La, Lb and Co). Above circuit is well-matched for no isolated ac-module applications because of the following advantages: 1) high efficiency over a wide load range by using MOSFETs for all active switches since their intrinsic body diodes are naturally inactive; 2) low ground leakage current because the voltage applied to the parasitic ground loop capacitance contains only low frequency components; 3) smaller output inductance as compared to that of the common full-bridge inverter with bipolar PWM switching; and 4) low-output ac current distortion because there is no need to have dead time for the proposed circuit since the three active switches in the same phase-leg never all turn ON during the same PWM cycle.

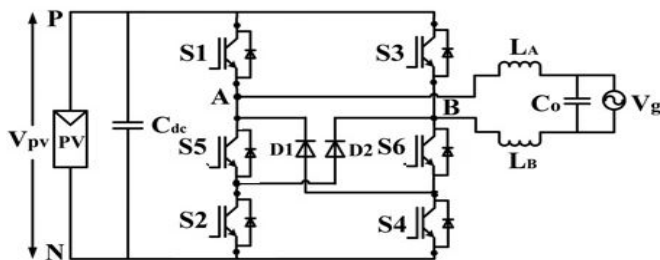


Fig.5 IGBT H6 type transformerless topology

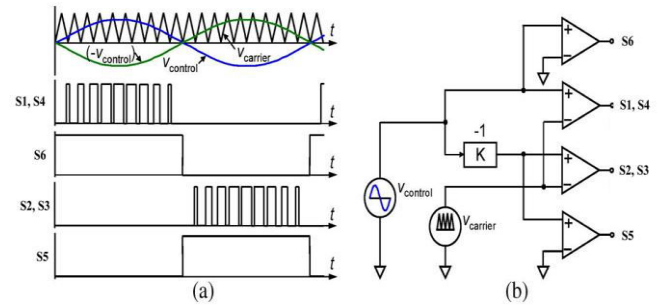


Fig. 6. PWM scheme for the proposed inverter: (a) signals in time domain; and (b) implemented circuit.

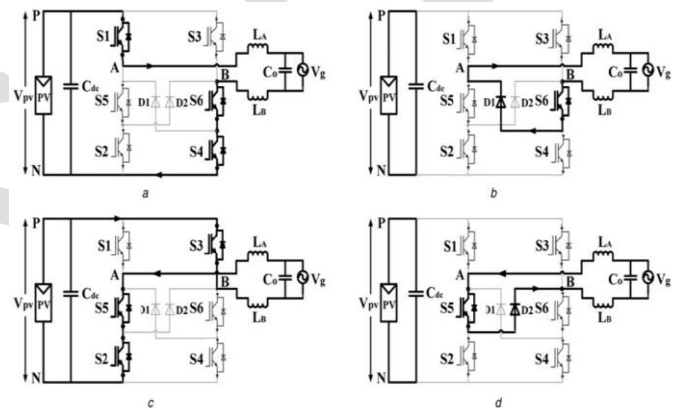


Fig.7 Operation of MOSFET H6 type topology

- a-Active
- b-Freewheeling mode in the positive half-cycle of grid current
- c- Active
- d-Freewheeling mode in the negative half-cycle of grid current

Fig. 6 shows that, the PWM structure scheme for the proposed inverter. As displayed in Fig. 6(a), the top device in one leg and the bottom device in the other leg are switched simultaneously in the PWM cycle and the middle device operates as a polarity selection switch in the grid cycle. As shown in Fig. 6(b), if the sinusoidal control voltage $v_{control}$, which is synchronized with output voltage, is higher than the triangular carrier voltage $v_{carrier}$, then the gating voltage G_1 and G_6 are active; otherwise, G_1 and G_6 are inactive. And if $v_{control}$ is higher than zero, the gating voltage G_4 is active; otherwise, G_4 is inactive. Similarly, the comparison of $(-v_{control})$ with $v_{carrier}$ or zero results in the logical signals to control G_2 , G_5 , and G_3 , respectively.

Fig. 7 shows the four topological stages in one grid cycle for the proposed inverter. Note that the point N is the dc-link negative terminal, and the point E is the grid

Paper ID: EE23

negative terminal the four operation modes are briefly described as follows. During the grid positive half cycle, switch S 4 remains ON, whereas S 1 , S 6 , and D 1 commutate at the PWM switching frequency. When S 1 , S 6 , and S 4 are ON and the other switches and diodes are OFF, the inductor current is charging, as shown in Fig. 7(a). Under the condition that the inductance values of L 1 and L 2 are identical, the inductor voltage can be found as

$$VL1=VL2=0.5(V_{dc}-V_{ac}). \tag{11}$$

And the output voltage vac is calculated by

$$V_{ac}=V_{dc}M\sin(\omega t) \tag{12}$$

where vdc is the dc-link voltage, M is the modulation index, and ω is the angular frequency of the grid. For simplification, the impedance at the line frequency between neutral line and ground is neglected. From (1) and (2), the ground potential shown in Fig. 7(a) in the charging interval during positive grid half cycle can be expressed

$$V_{en1}=0.5V_{dc}[1-(M\sin(\omega t))]. \tag{13}$$

the free wheel in g interval during the positive grid half cycle shown in Fig. 7(b), the S 1 and S 6 simultaneously turn OFF and S 4 and D 1 are ON. The voltages of the inductor L 1 and L 2 are given as

$$VL1=VL2=-0.5V_{ac} \tag{14}$$

Under the condition that the S 1 and S 6 share the dc-link voltage when they are simultaneously turned off, the voltage

Stress of the S 6 can be found as

$$VS6=0.5V_{dc} . \tag{15}$$

For simplification, the impedance at the line frequency between neutral line and ground is also neglected. From (2), (4), and (5), the ground potential shown in Fig.7 (b) in the freewheeling interval during positive grid half cycle can be expressed as

$$V_{en2}=0.5V_{dc}[1-(M\sin(\omega t))]. \tag{16}$$

On the basis of the fact that (6) is identical to (3), the PWM Switching frequency voltage of the ground potential is avoided. The operation modes similarly change during the grid negative half cycle. From Fig. 5(a) (d), it can be seen that the body diodes of the MOSFETs are naturally inactive and the high-frequency voltage of the ground potential is avoided during the whole grid cycle. As a result,

MOSFETs can be employed as all the active switches to achieve higher efficiency than that of the five-switch inverter, and high ground leakage current can be avoided just as same as the five-switch inverter.

IV. MATLAB SIMULATION OF PROPOSED TOPOLOGY

Simulation of proposed topology is as shown in the following fig. and also the matlab simulation of pulse width modulation.

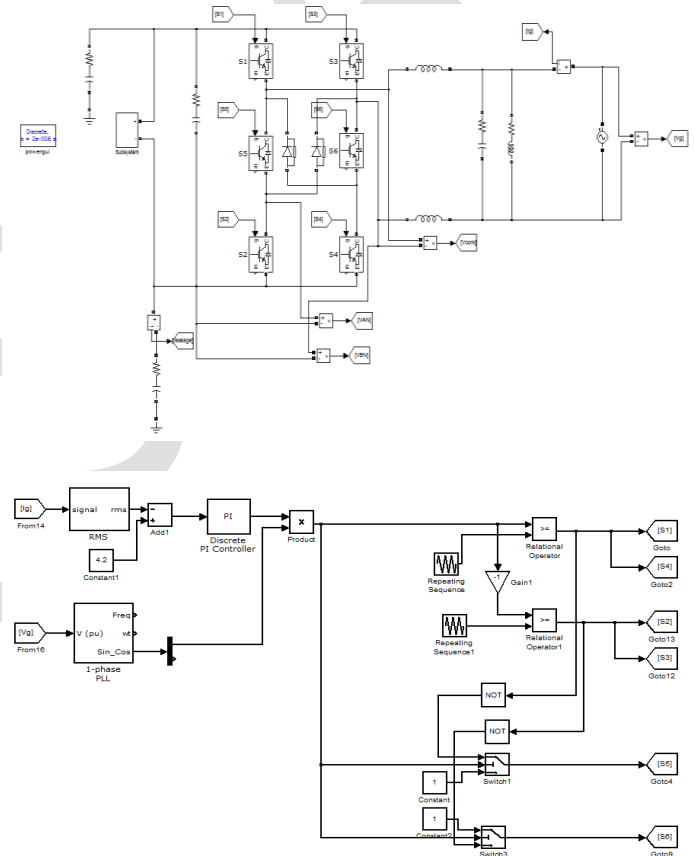


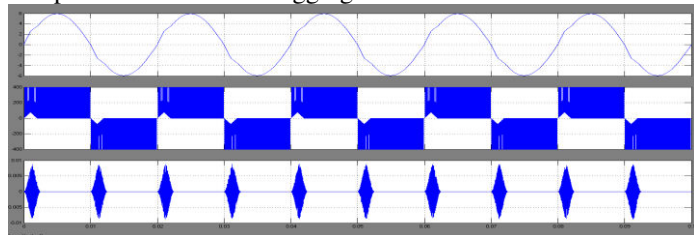
Fig.8 MATLAB model of H6 type IGBT inverter and PWM scheme.

V. V RESULT ANALYSIS

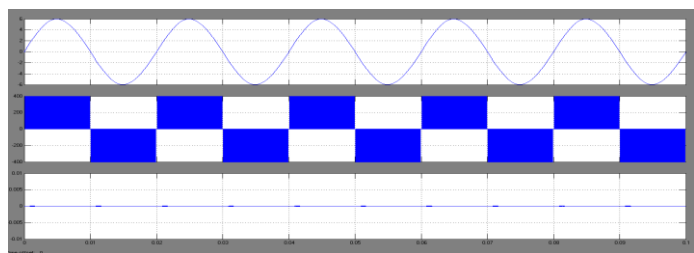
This simulation results are carried out by using the matlab Simulink software for to compare the operation and analyze and to check overall performance of the H6 type IGBT and MOSFET transformer less grid connected single phase grid connected PV system. The parameters used for the both two topologies are same. PV module and the stray capacitor between the PV module and ground replaced with

Paper ID: EE23

400 V dc source and two capacitors of 75nf each respectively. The grid line voltage is 230 V with frequency is 50 Hz and the switching frequency of switches is 20 kHz and power factor is 0.95 lagging.



A



B

Fig. Waveform of Grid current upper, DM voltage middle and leakage current lower.

A H6 type MOSFET topology
B H6 type IGBT topology

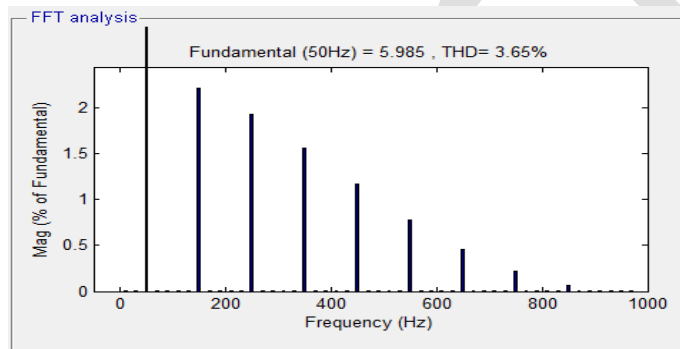
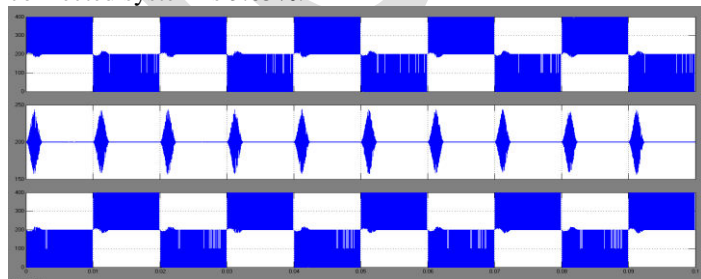
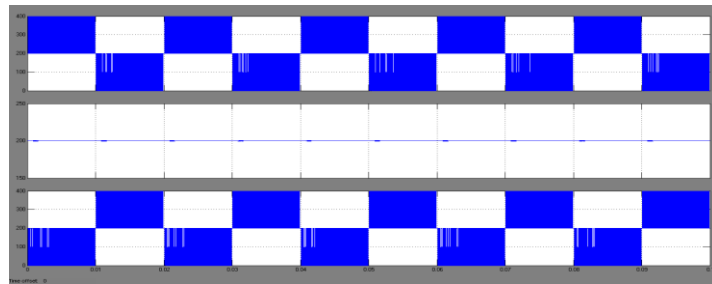


Fig. FFT analysis of H6 type MOSFET topology
The THD of H6 type MOSFET topologies with grid connected system is 3.65%.



A



B

Fig. waveform of Van upper, Van middle, Vbn lower.

A H6 MOSFET topology
B H6 type IGBT topology

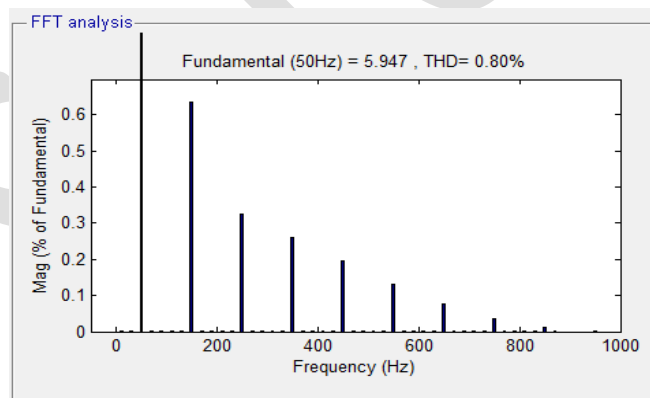


Fig. FFT analysis of H6 type IGBT topology
The THD of above topology is 0.80%

VI. CONCLUSION

This paper proposes a H6 type IGBT transformer less topology for a single-phase grid connected PV system. This paper presents the performance of two H6 type topologies and compared with their simulation results. IGBT topology has following advantages over the MOSFET topology:

- 1 Leakage current is reduced as compared with the traditional one.
- 2 Excellent DM characteristics can be achieved by using the IGBT topology.
- 3 CM voltage characteristics achieved by IGBT topology as compared with the MOSFET topology.
- 4 The THD of proposed topology have lower than the MOSFET topology.

REFERENCES

- [1] M. Calais, J. Myrzik, T. Spooner, and V. G. Agelidis, "Inverters for single phase grid connected photovoltaic systems—An overview," in Proc. IEEE PESC, 2002, vol. 2, pp. 1995–2000.
- [2] F. Blaabjerg, Z. Chen, and S. B. Kjaer, "Power electronics as efficient interface in dispersed power generation systems," IEEE Trans. Power Electron., vol. 19, no. 5, pp. 1184–1194, Sep. 2004.
- [3] S. B. Kjaer, J. K. Pedersen, and F. Blaabjerg, "A review of single-phase grid-connected inverters for photovoltaic modules," IEEE Trans. Ind. Appl., vol. 41, no. 5, p. 1292, Sep./Oct. 2005.
- [4] Quan Li and P. Wolfs, "A review of the single phase photovoltaic module integrated converter topologies with three different dc link configurations," IEEE Trans. Power Electron., vol. 23, no. 3, pp. 1320–1333, May 2008.
- [5] M. Fornage, "Method and apparatus for converting direct current to alternating current," U.S. Patent applications 0 221 267 A1, Sep. 27, 2007.
- [6] S. Saha and V. P. Sundarsingh, "Novel grid-connected photovoltaic inverter," Proc. Inst. Elect. Eng., vol. 143, pp. 219–224, Mar. 1996.
- [7] A. Lohner, T. Meyer, and A. Nagel, "A new panel-integratable inverter concept for grid-connected photovoltaic systems," in Proc. IEEE ISIE, 1996, vol. 2, pp. 827–831.
- [8] S. B. Kjaer and F. Blaabjerg, "Design optimization of a single phase inverter for photovoltaic applications," in Proc. IEEE PESC, 2003, vol. 3, pp. 1183–1190.
- [9] A. C. Kyritsis, E. C. Tatakis, and N. P. Papanikolaou, "Optimum design of the current-source flyback inverter for decentralized grid-connected photovoltaic systems," IEEE Trans. Energy Convers., vol. 23, no. 1, pp. 281–293, Mar. 2008.
- [10] B. Sahan, A. N. Vergara, N. Henze, A. Engler, and P. Zachari as, "A single-stage PV module integrated converter based on a low-power current-source inverter," IEEE Trans. Ind. Electron., vol. 55, no. 7, pp. 2602–2609, Jul. 2008.
- [11] H. Patel and V. Agarwal, "A single-stage single-phase transformer-less doubly rounded grid-connected PV interface," IEEE Trans. Energy Convers., vol. 24, no. 1, pp. 93–101, Mar. 2009.
- [12] S. Funabiki, T. Tanaka, and T. Nishi, "A new buck-boost-operation-based sinusoidal inverter circuit," in Proc. IEEE PESC, 2002, pp. 1624–1629.
- [13] J. M. Chang, W. N. Chang, and S. J. Chiang, "Single-phase grid-connected PV system using three-arm rectifier-inverter," IEEE Trans. Aerosp. Electron. Syst., vol. 42, no. 1, pp. 211–219, Jan. 2006.
- [14] A. C. Kyritsis, N. P. Papanikolaou, and E. C. Tatakis, "Enhanced current pulsation smoothing parallel active filter for single stage grid-connected AC-PV modules," in Proc. IEEE (EPE-PEMC, Sep. 1–3, 2008, pp. 1287–1292.
- [15] T. Shimizu, K. Wada, and N. Nakamura, "Flyback-type single-phase utility interactive inverter with power pulsation decoupling on the dc input for an ac photovoltaic module system," IEEE Trans. Power Electron., vol. 21, no. 5, pp. 1264–1272, Sep. 2006.
- [16] P. T. Krein and R. S. Balog, "Cost-effective hundred-year life for single-phase inverters and rectifiers in solar and LED lighting applications based on minimum capacitance requirements and a ripple power port," in Proc. IEEE APEC, Washington, DC, Feb. 15–19, 2009, pp. 620–625.
- [17] Q. Li and P. Wolfs, "A current fed two-inductor boost converter with an integrated magnetic structure and passive lossless snubbers for photovoltaic module integrated converter applications," IEEE Trans. Power Electron., vol. 22, no. 1, pp. 309–320, Jan. 2007.
- [18] M. Andersen and B. Alvsten, "200 W low cost module integrated utility interface for modular photovoltaic energy systems," in Proc. IEEE IECON, 1995, pp. 572–577.
- [19] C. Rodriguez and G. Amaratunga, "Long-lifetime power inverter for photovoltaic AC modules," IEEE Trans. Ind. Electron., vol. 55, no. 7, pp. 2593–2601, Jul. 2008.
- [20] W. Yu, C. Hutchens, J.-S. Lai, J. Zhang, G. Lisi, A. Djabbari, G. Smith, and T. Hegarty, "High efficiency converter with charge pump and coupled inductor for wide input photovoltaic ac module applications," in Proc. IEEE ECCE, San Jose, CA, Sep. 20–24, 2009, pp. 3895–3900.
- [21] M. Victor, F. Greizer, S. Bremicker, and U. Hubler, "Method of converting a direct current voltage of a source of direct current voltage, more specifically of a photovoltaic source of direct current voltage, into an alternating current voltage," U.S. Patent 0 286 281 A1, Dec. 29, 2005.
- [22] H. Akagi and T. Shimizu, "Attenuation of conducted EMI emissions from an inverter-driven motor," IEEE Trans. Power Electron., vol. 23, no. 1, pp. 282–290, Jan. 2008.
- [23] R. Gonzalez, E. Gubia, J. Lopez, and L. Marroyo, "Transformerless single-phase multi level based photovoltaic inverter," IEEE Trans. Ind. Electron., vol. 55, no. 7, pp. 2694–2702, Jul. 2008.